

Supporting Information

Experimental and Theoretical Insights into Light Confinement within 2D Waveguides of Alkylphenyl Benzothiadiazole Crystals

Iván Torres-Moya^a, Mohammad Afsar Uddin^b, Sergio Gámez-Valenzuela^c, Javier Álvarez-Conde^d, Juan Cabanillas-González^d, Ana L. Montero-Alejo^e, Ana M. Rodríguez^a, Luis A. Montero-Cabrera^f, M. Carmen Ruiz Delgado^{*c,g}, Berta Gómez-Lor^{*b}, Pilar Prieto^{*a}.

^a Department of Inorganic, Organic Chemistry and Biochemistry, Faculty of Chemical Science and Technologies, University of Castilla-La Mancha (UCLM)-IRICA, 13071 Ciudad Real, Spain.

^b Institute of Materials Science of Madrid (ICMM-CSIC), Sor Juana Inés de la Cruz 3, Cantoblanco, 28049 Madrid, Spain.

^c Department of Physical Chemistry, University of Málaga, Campus de Teatinos s/n, 29071 Málaga, Spain

^d Madrid Institute for Advanced Studies, IMDEA Nanociencia, Calle Faraday 9, Ciudad Universitaria de Cantoblanco, 28049 Madrid, Spain.

^e Departamento de física, Facultad de Ciencias Naturales, Matemática y del Medio Ambiente (FCNMM), Universidad Tecnológica Metropolitana; Ñuñoa, 7800002 Santiago, Chile.

^f Computational and Theoretical Chemistry Laboratory, Department of Physical Chemistry, Faculty of Chemistry, University of Havana, 10400 Havana, Cuba.

^g Instituto Universitario de Materiales y Nanotecnología, IMANA, University of Málaga, Campus de Teatinos, 29071, Málaga, Spain.

List of contents	Page
1. Experimental details	S3
1.1. ^1H-NMR and ^{13}C-NMR spectra	S3
2. HRSEM images	S4
3. Optical waveguiding behaviour	S5
4. Single crystal X-ray structure	S7
5. Binding energy	S13
6. TD-DFT analysis	S14
7. Transition dipole moment analysis	S17

1. Experimental details

1.1. ^1H -NMR and ^{13}C -NMR spectra

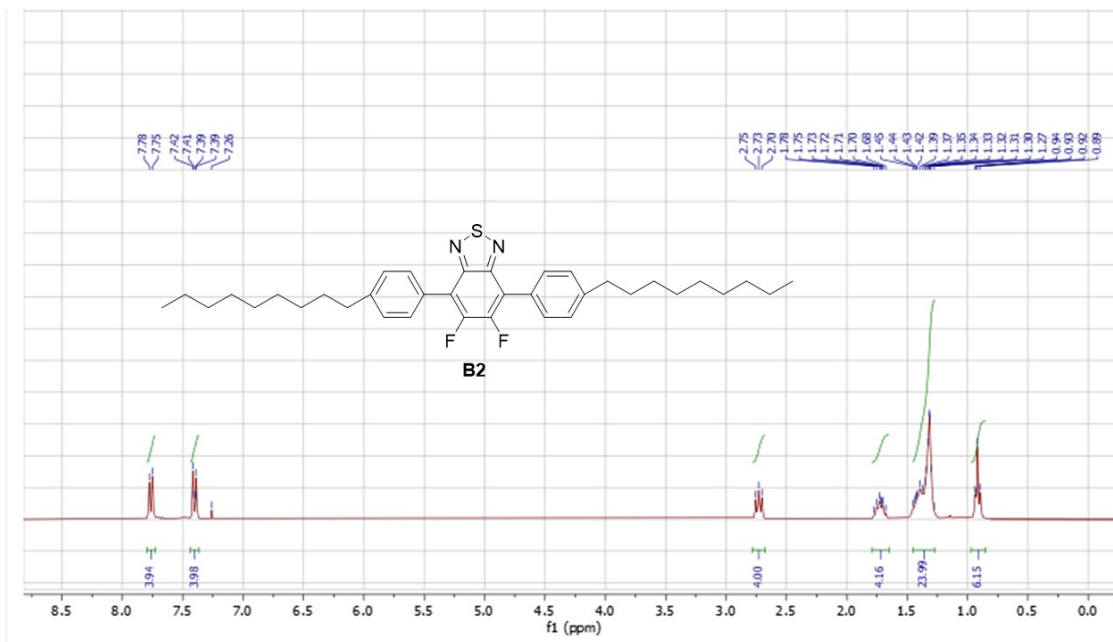


Figure S1. ^1H NMR (300MHz, CDCl_3) spectrum for **B2**.

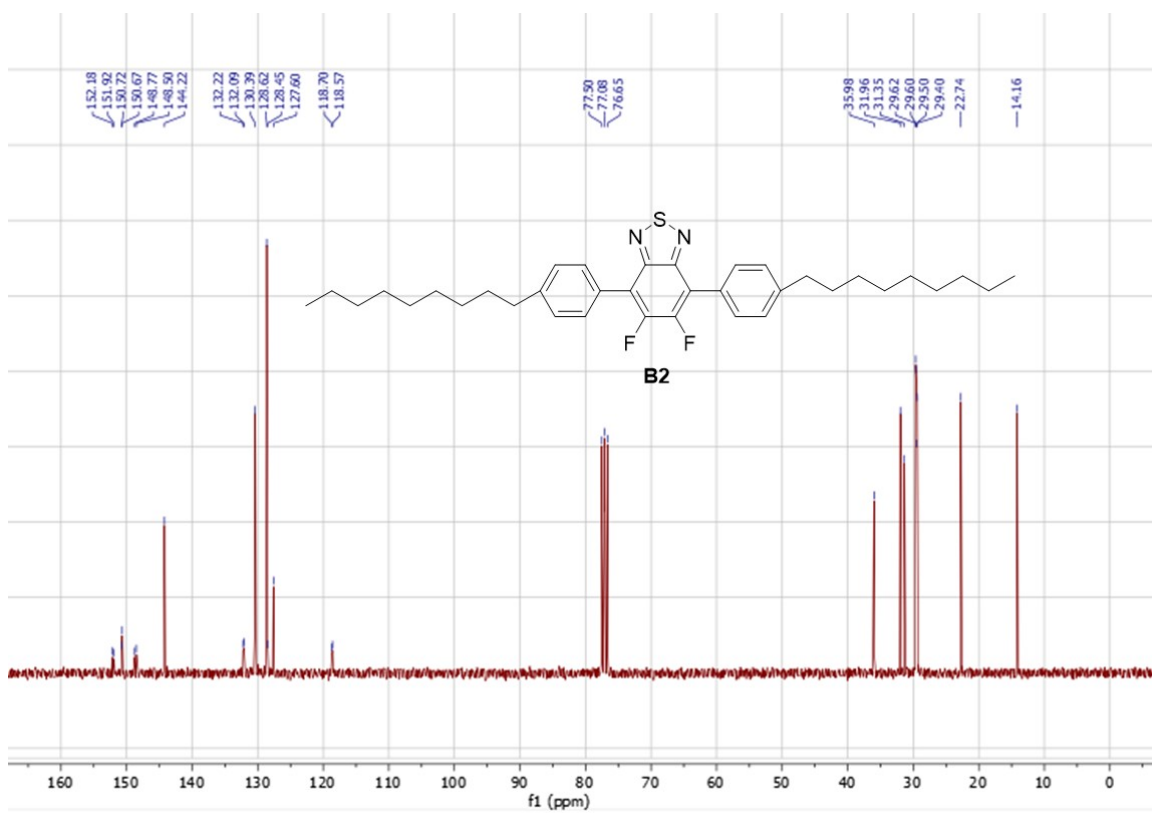


Figure S2. ^{13}C NMR (300MHz, CDCl_3) spectrum for **B2**.

2. HRSEM images

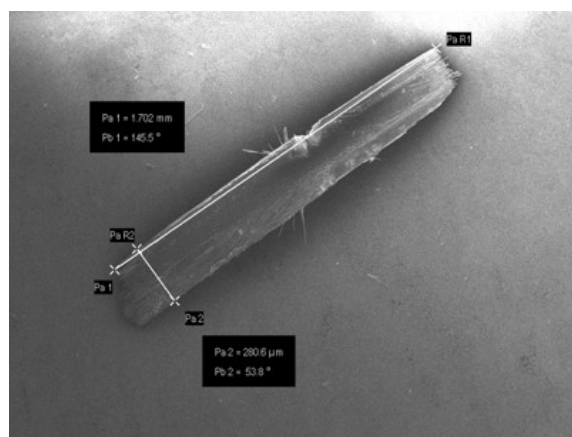


Figure S3. HRSEM image (298 K, glass substrate) of crystals formed by the self-assembly of **B1** in $\text{CHCl}_3/\text{CH}_3\text{CN}$ solvent mixture.

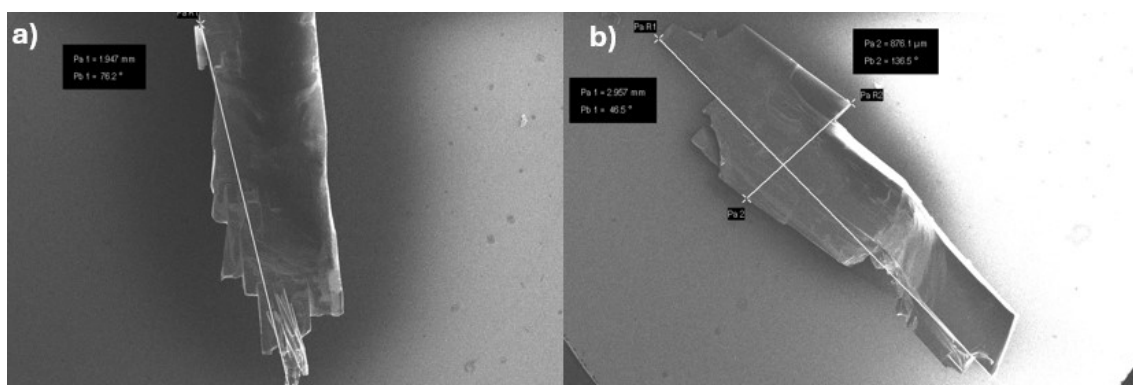


Figure S4. HRSEM images (298 K, glass substrate) of crystals formed by the self-assembly of **B2** in (a) $\text{CHCl}_3/\text{CH}_3\text{CN}$ and (b) THF/MeOH solvent mixtures.

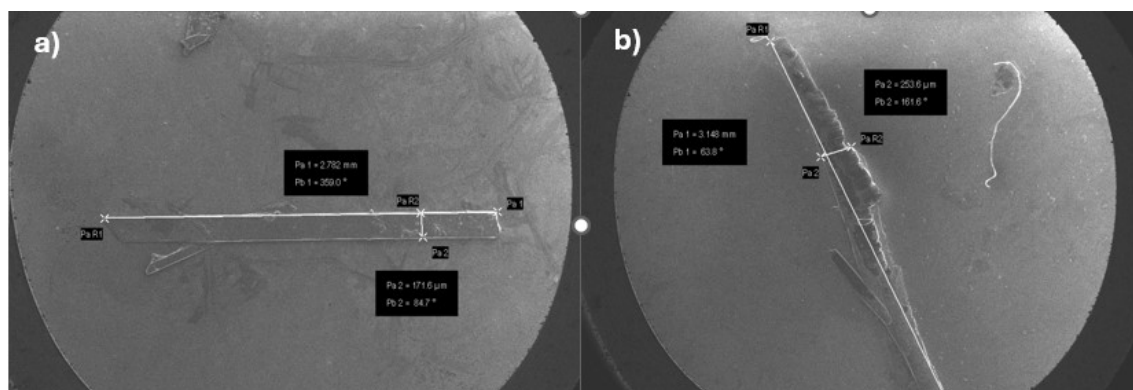


Figure S5. HRSEM images (298 K, glass substrate) of crystals formed by the self-assembly of **B3** in (a) $\text{CHCl}_3/\text{EtOH}$ and (b) THF/MeOH solvent mixtures.

3. Optical waveguiding behaviour

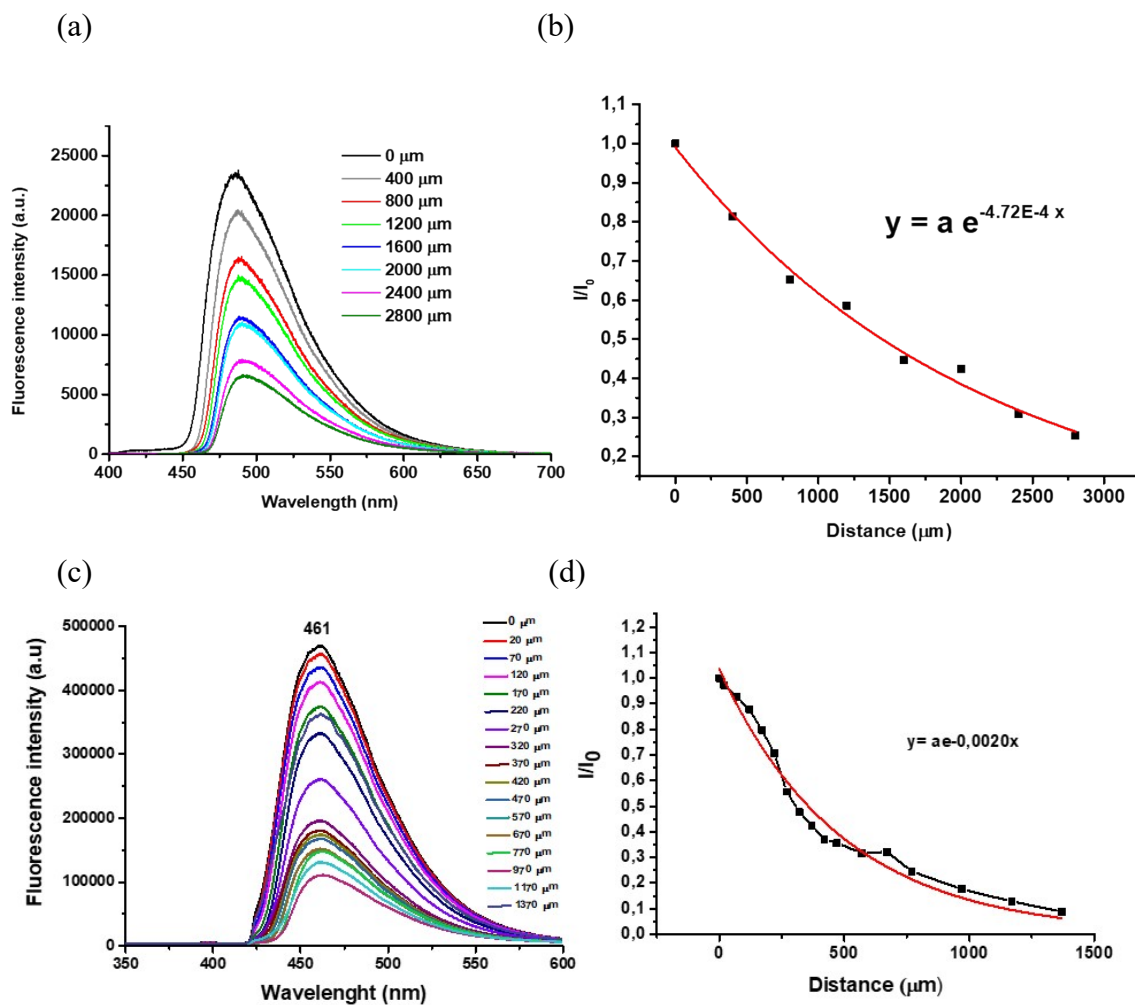


Figure S6. (a) Photoluminescence (PL) spectra collected at the crystal tip of **B1** as the distance between the excitation point and the crystal tip increases along the y-axis. (b) Ratio of PL intensities at the initial (I_0) and intermediate (I) positions along the fiber as a function of distance. Red lines represent exponential fits for **B1**. (c) PL spectra collected at the crystal tip of **B1** upon varying the distances between the excitation point and the crystal tip along the x-axis. (d) Corresponding I_0/I ratio as a function of distance, with red lines indicating exponential decay fits. In all cases, crystals were photoexcited at 355 nm.

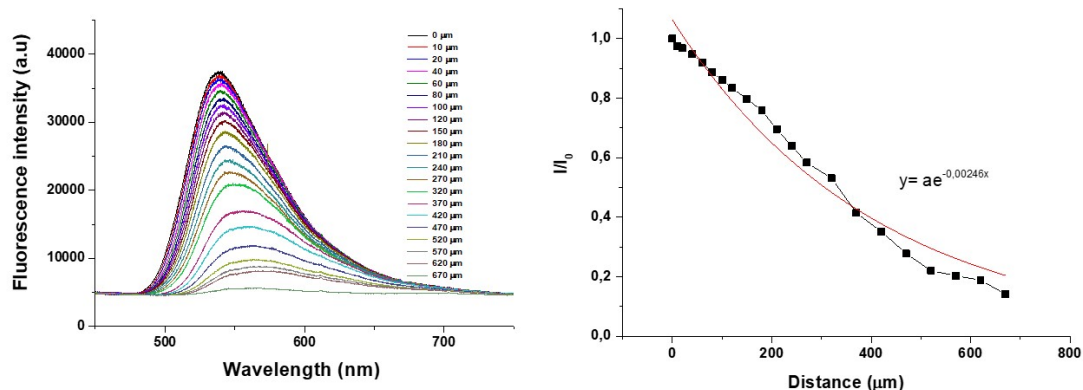


Figure S7. PL spectra of crystals collected at the tip upon varying the distance between the excitation point and the crystal tip of **B3** (left). The ratio of PL intensities at the initial (I_0) and intermediate (I) positions along the fiber as a function of distance (right). Red lines represent fits to exponential decay models for **B3**. Crystals were photoexcited at 355 nm.

4. Single crystal X-ray structure

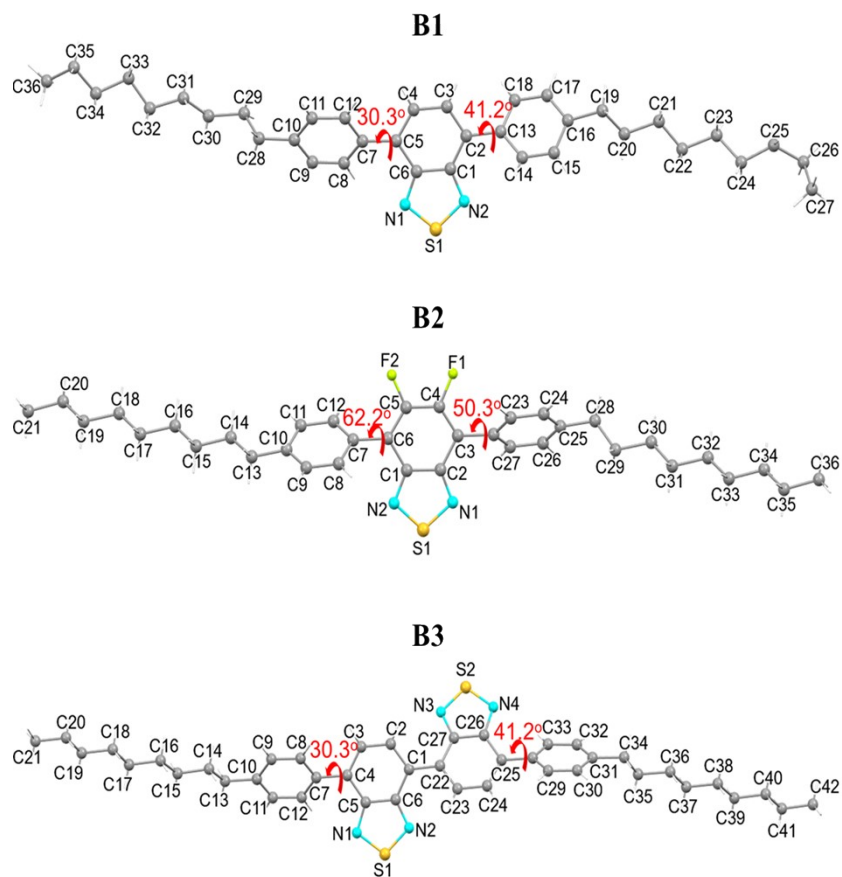
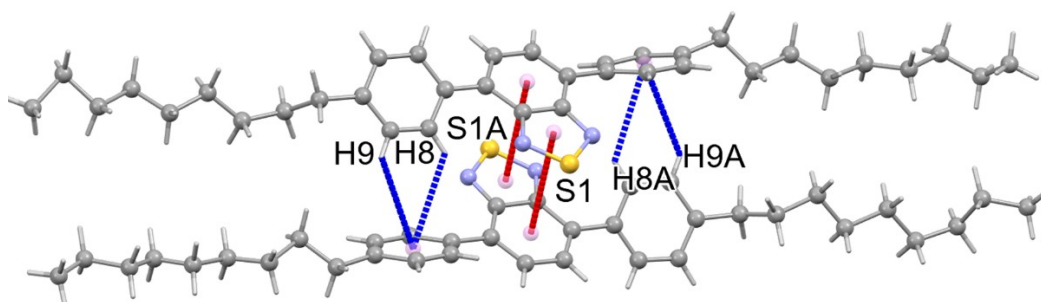
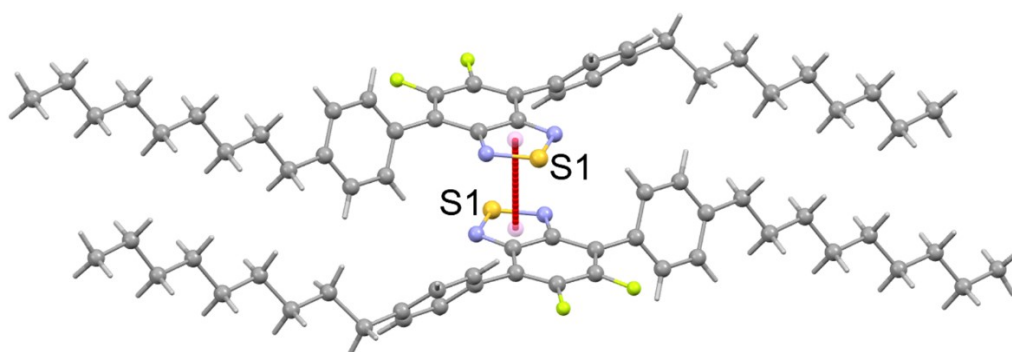


Figure S8. Molecular structure of compounds **B1**, **B2** and **B3** with the adopted labelling scheme.

(a)



(b)



(c)

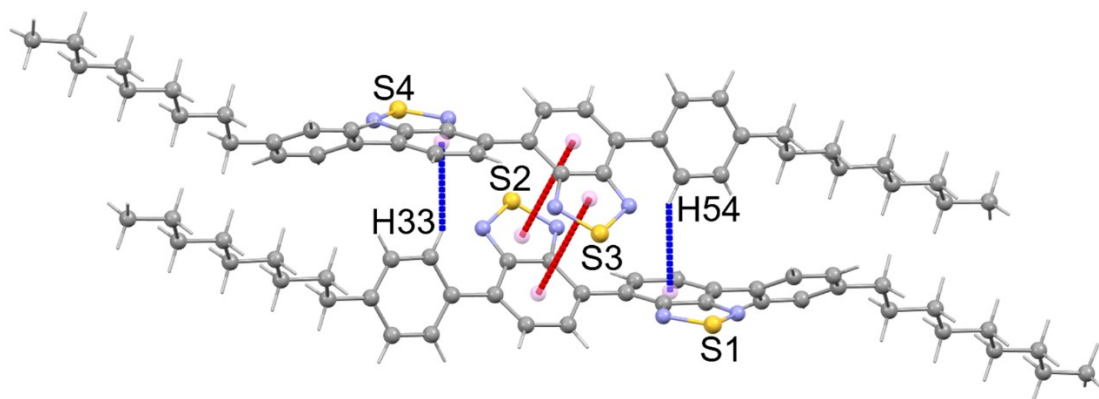


Figure S9. Dimers formation for compounds (a) **B1**, (b) **B2** and (c) **B3** through π - π (red color) and CH- π (blue color) interactions.

Table S1. Structural parameters characterizing the non-covalent interactions in compounds **B1**, **B2**, and **B3**. Ct denotes the ring centroid. The angle β corresponds to the angle between the H-centroid vector and the H-plane lines in CH $\cdots\pi$ interaction, and to the angle between the centroid-centroid vector and the centroid-plane in π - π stacking interactions.

CH\cdotsF interactions				
Compound	DH \cdots A	d(H \cdots A) (Å)	d(D \cdots A) (Å)	α (DHA) (°)
B2	C14-H14B \cdots F2	2.72	3.64	156.3
	C24-H24 \cdots F1	2.93	3.29	104.3
Chalcogen bonding				
B1	S1-N2A	3.51		
	S1A-N2	3.48		
B2	S1-N2	3.68		
B3	S1-N3	3.31		
	S2-N2	3.27		
	S3-N8	3.28		
	S4-N6	3.33		
	S5-N11	3.23		
	S6-N9	3.21		
	S7-N16	3.28		
	S8-N14	3.33		
	S9-N20	3.26		
	S10-N18	3.22		
CH$\cdots\pi$ interaction				
	Groups	d (H-Ct) (Å)	d(H-plane) (Å)	β (°)
B1	C3H3 \cdots (C13A-C17A)	3.31	2.86	30.2
	C8H8 \cdots (C13A-C18A)	3.16	2.93	22.0
	C9-H9 \cdots (C13A-C18A)	3.25	3.06	19.7
	C12H12 \cdots (C1A-C6A)	2.92	2.88	9.5
	C8AH8A \cdots (C13-C18)	3.21	2.91	25.0
	C9A-H9A \cdots (C13-C18)	3.25	3.11	16.9
	C4A-H4A \cdots (C1-C6)	3.12	3.09	7.9
B2	C12-H12 \cdots (C22-C27)	3.10	3.06	9.2
	C24-H24 \cdots (C1-C6)	3.29	2.95	26.3
	C24-H24 \cdots (S1-N2)	3.03	2.94	14.0
B3	C23-H23 \cdots (C1-C6)	3.04	2.88	18.7
	C29-H29 \cdots (C7-C12)	3.02	2.97	10.4
	C33-H33 \cdots (C64-C69)	2.79	2.78	4.8
	C50-H50 \cdots (C91-C96)	3.02	2.97	10.4
	C66-H66 \cdots (C106-C111)	3.24	2.91	26.1
	C72-H72 \cdots (C112-C117)	3.20	3.14	11.1
	C86-H86 \cdots (C43-C48)	3.31	2.93	27.7
	C95-H95 \cdots (C49-C54)	3.30	3.22	12.6
	C54-H54 \cdots (C1-C6)	2.79	2.78	4.8
	C44-H44 \cdots (C85-C90)	3.05	2.89	39.0

	C107-H107...(C64-C69)	3.12	2.89	22.1
	C113-H113...(C70-C75)	3.04	3.01	8.1
	C117-H117...C148-C153)	2.80	2.78	22.7
	C129-H129...(C169-C174)	3.27	2.97	24.7
	C135-H135...(C175-C180)	3.04	2.93	23.4
	C138-H138...(C85-C90)	2.79	2.77	6.9
	C149-H149...(C190-C195)	2.92	2.75	19.6
	C155-H155...(C196-C201)	3.10	2.99	15.3
	C170-H170...(C127-C132)	2.94	2.76	20.1
	C176-H170...(C133-C138)	3.08	2.99	13.9
	C192-H192...(C148-C153)	3.27	2.99	23.9
	C197-H197...(C169-C174)	2.77	2.75	6.9
	C200-H200...(C154-C159)	3.07	3.01	11.3
	C203-H20E...(C175-C180)	3.37	3.34	7.6
$\pi\cdots\pi$ stacking				
	Groups	d(Ct-Ct) (Å)	d(Ct-Plane) (Å)	β (°)
B1	(S1-N2)...(C1A-C6A)	3.72	3.51	19.3
	(C1-C6)...(S1A-N2A)	3.66	3.47	18.5
B2	(S1-N2)...(S1-N2)	3.45	3.40	9.8
B3	(S2-N3)...(C43-C48)	3.66	3.33	24.5
	(S3-N6)...(C22-C27)	3.66	3.35	23.7
	(S6-N12)...(C127-C132)	3.67	3.34	24.5
	(S7-N14)...(C106-C111)	3.70	3.37	24.4
	(S10-N20)...(C190-C195)	3.71	3.36	25.1
S$\cdots\pi$ interaction				
	Groups	d(S-Ct) (Å)	α (Ct(Ph)-S-Ct(BTD)) (°)	
B1	S1...(C7-C12)	3.40	115.5	
	S1A...(C7A-C12A)	3.49	116.7	
B2	S1...(C7-C12)	3.53	165.3	
B3	S1...(C51-54)	3.93	140.0	
	S4...(C29-C33)	3.90	140.2	
	S5...(C134-C138)	3.94	136.8	
	S8...(C112-C116)	3.83	140.5	
	S9...(C196-C199)	3.84	137.7	
F$\cdots\pi$ interaction				
	Groups	d(F-Ct) (Å)	d(F...plane) (Å)	β (°)
B2	F1...(C1-C6)	3.71	3.40	23.6
	F1...(C22-C27)	4.12	2.43	53.8

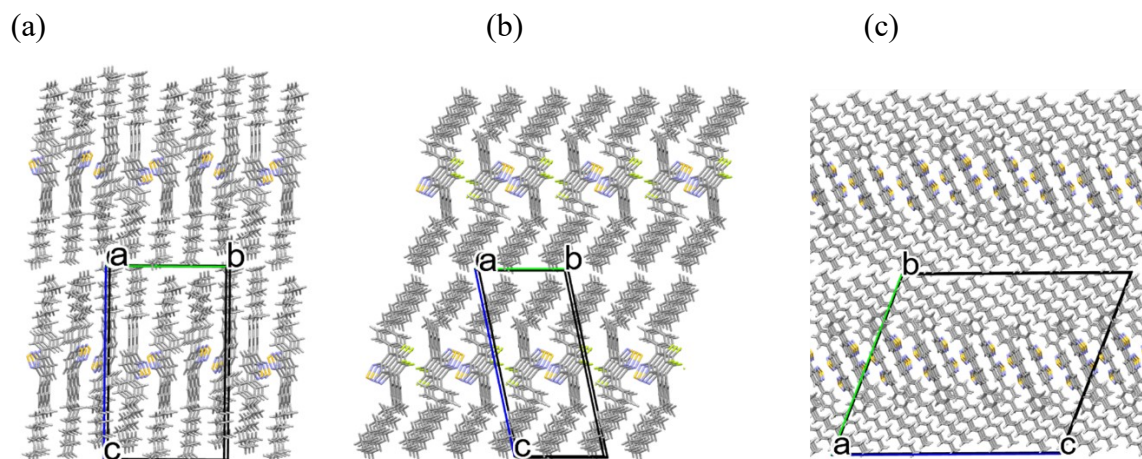


Figure S10. Crystal packing of compounds (a) **B1**, (b) **B2** and (c) **B3** viewed along the *a*-axis, showing their lamellar arrangement.

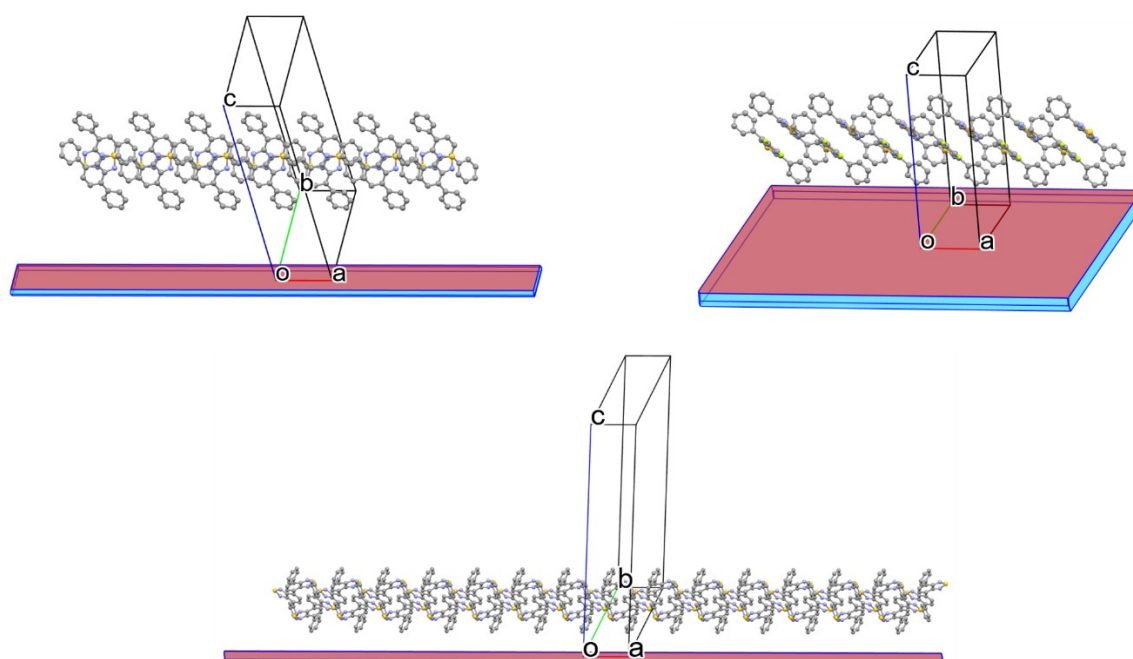


Figure S11. Predicted crystal morphologies of compounds **B1**, **B2** and **B3** generated using the Visual Habit tool in the Mercury software.

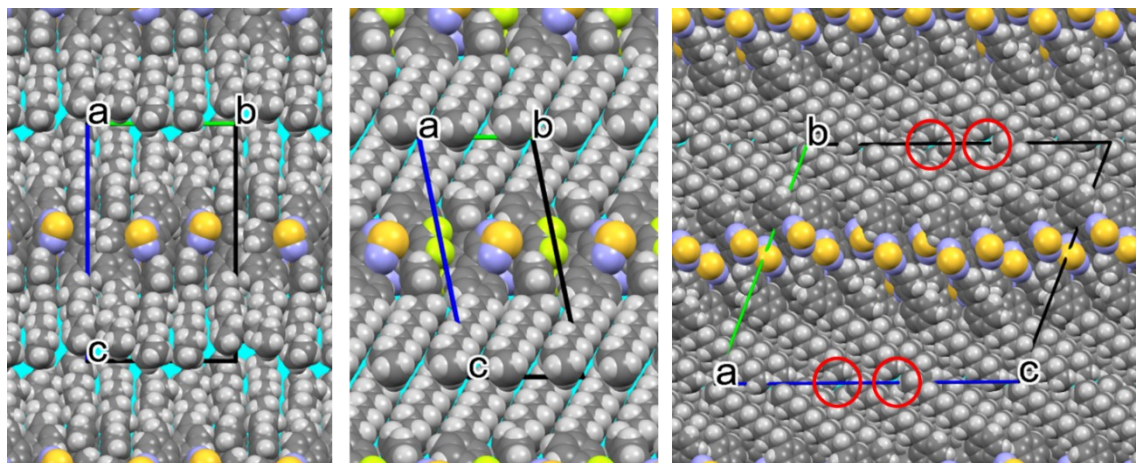


Figure S12. Space-filling representation of the structure packing for **B1**, **B2** and **B3** showing microchannels (light blue color) aligned along $[100]$ direction. The microchannels of **B3** are marked with red circles.

5. Binding energy

Table S2. Calculated exciton energies (E) for the lowest energy singlet states (S_n) of molecules **B1**, **B2** and **B3** together with their respective Coulomb – exchange terms (E^{CE}) and oscillator strengths (f) after [4nCIS CNDOL/1CS| ω B97XD/6-31G**] modeling. Energies in eV.

Mol.	TD-DFT (ω B97XD/6-31G**)			CNDOL/1CS 4nCIS				Exp. (CH ₂ Cl ₂) ³⁶		
	E(eV)	λ (nm)	f	E(eV)	λ (nm)	f	E ^{CE} (eV)	E _{abs.} (eV)	E _{lum.} (eV)	λ (nm)
B1				2.58	480	0	3.23		2.43	510
				3.03	410	0	2.85			
	3.51	353	0.523	3.38	367	0.364	2.81	3.19		389
				3.96	313	0	2.86			
				4.07	305	0.001	3.12	3.94		315
				4.20	296	0	2.73			
	4.60	270	0.222	4.63	268	0.030	2.89	4.52		274
	TD-DFT (ω B97XD/6-31G**)			CNDOL/1CS 4nCIS				exp (CHCl ₃)		
	E(eV)	λ (nm)	f	E(eV)	λ (nm)	f	E ^{CE} (eV)	E _{abs.} (eV)	E _{lum.} (eV)	λ (nm)
B2				2.64	470	0	2.75		2.57	482
				3.12	397	0	2.66			
	3.5	354	0.545	3.35	370	0.312	2.77	3.35		370
				4.05	306	0.002	2.56	3.9		318
				4.23	293	0.001	2.67			
				4.41	282	0.002	2.72			
	4.51	275	0.269	4.65	267	0.035	2.74	4.61		269
	TD-DFT (ω B97XD/6-31G**)			CNDOL/1CS 4nCIS				Exp. (CH ₂ Cl ₂) ³⁷		
	E(eV)	λ (nm)	f	E(eV)	λ (nm)	f	E ^{CE} (eV)	E _{abs.} (eV)	E _{lum.} (eV)	λ (nm)
B3				2.55	486	0	2.61		2.43	511
				2.67	464	0	2.56			
	3.28	378	0.9401	3.04	408	0.184	2.62	3.02		410
				3.05	407	0.012	2.64			
	3.67	337	0.0022	3.15	394	0.397	2.66	4.00		310
				3.55	349	0.002	2.66			
				3.81	326	0	2.72			
				3.96	313	0	2.58			
				3.97	312	0.020	2.53			
				4.12	301	0	2.36			
			4.15	299	0.010	2.55				
4.44	279	0.0039	4.29	289	0.017	2.39	4.51		275	

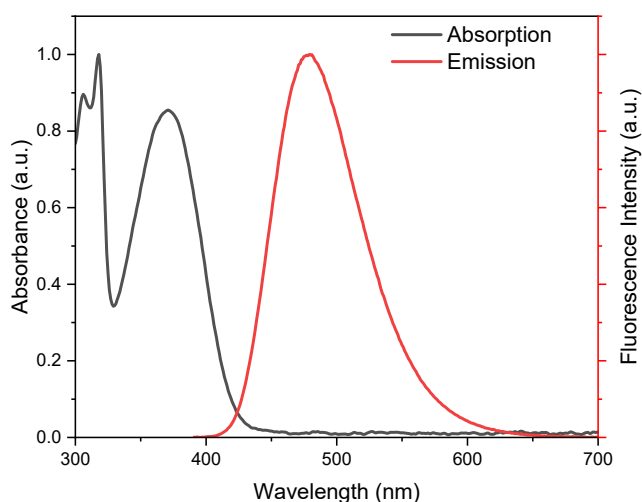


Figure S13. Absorption and emission spectra of **B2** in chloroform.

6. TD-DFT analysis

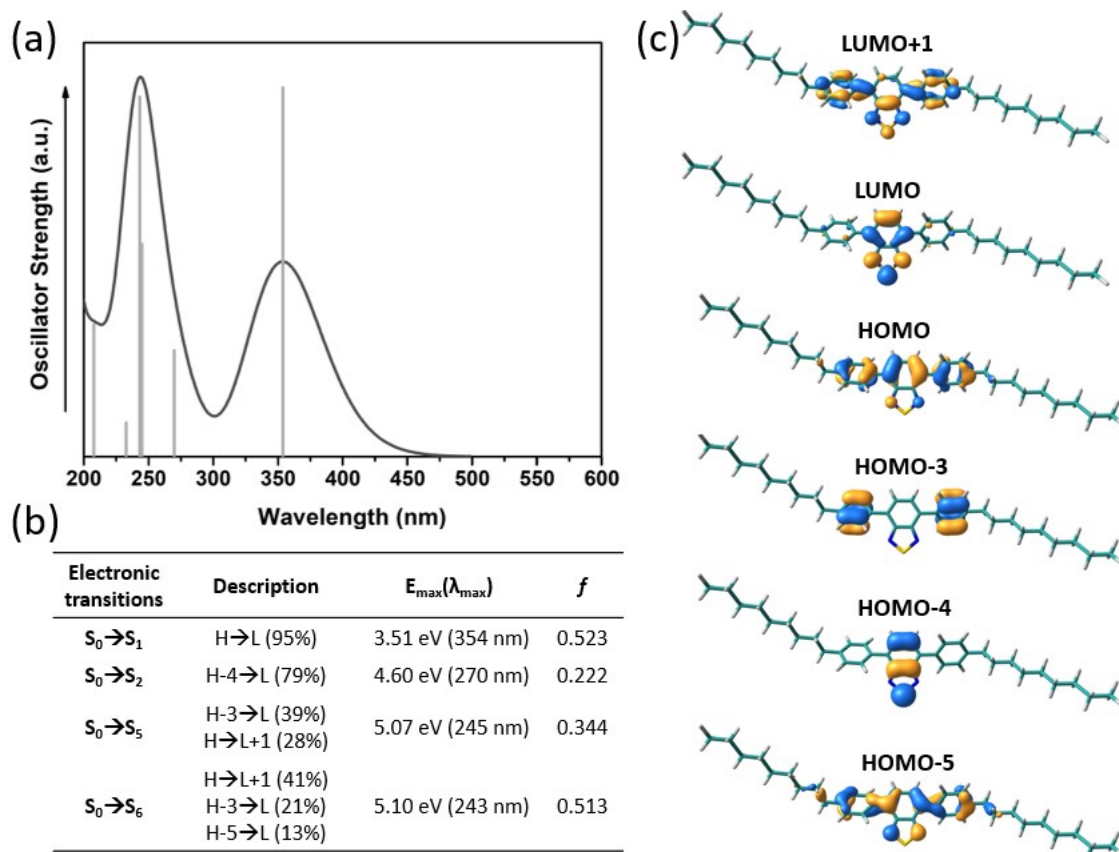


Figure S14. (a) Simulated absorption spectrum of an isolated **B1** molecule obtained from TD-DFT calculations at the ω B97X-D/6-31G** level, with vertical electronic transitions shown as grey lines. (b) Summary of the main electronic transitions contributing to the

absorption features. (c) Topologies of the molecular orbitals involved in the main electronic transitions.

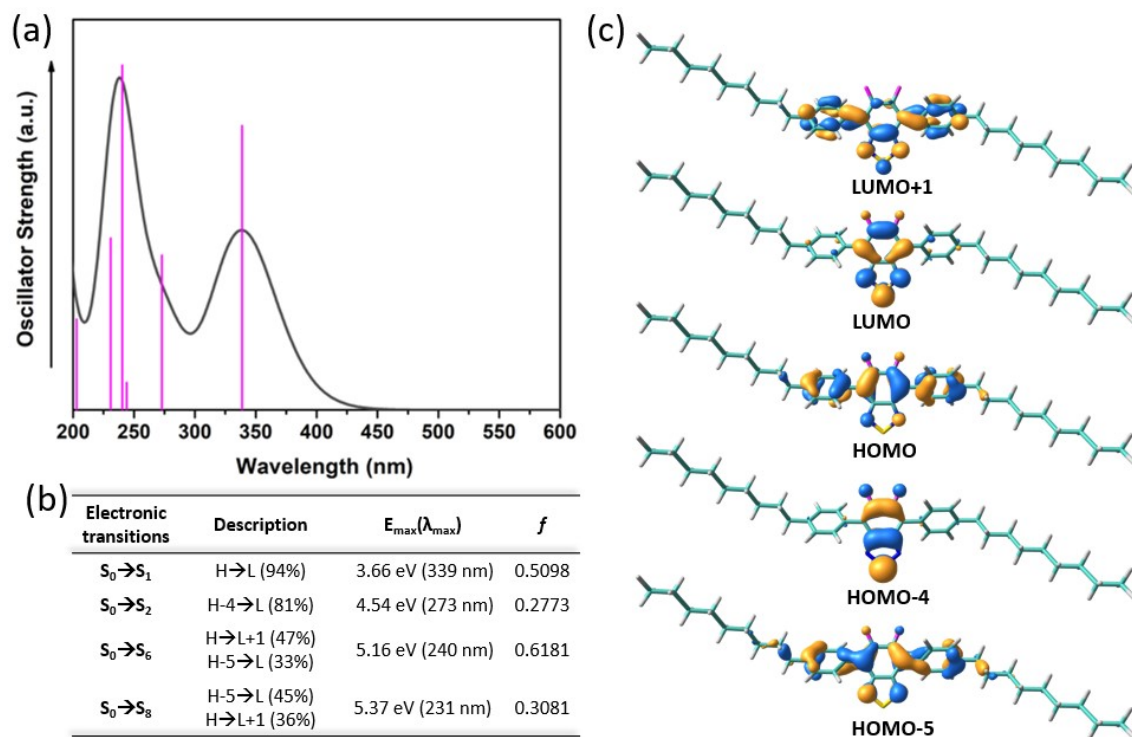


Figure S15. (a) Simulated absorption spectrum of an isolated **B2** molecule obtained from TD-DFT calculations at the ω B97X-D/6-31G** level, with vertical electronic transitions shown as pink lines. (b) Summary of the main electronic transitions contributing to the absorption features. (c) Topologies of the molecular orbitals involved in the main electronic transitions.

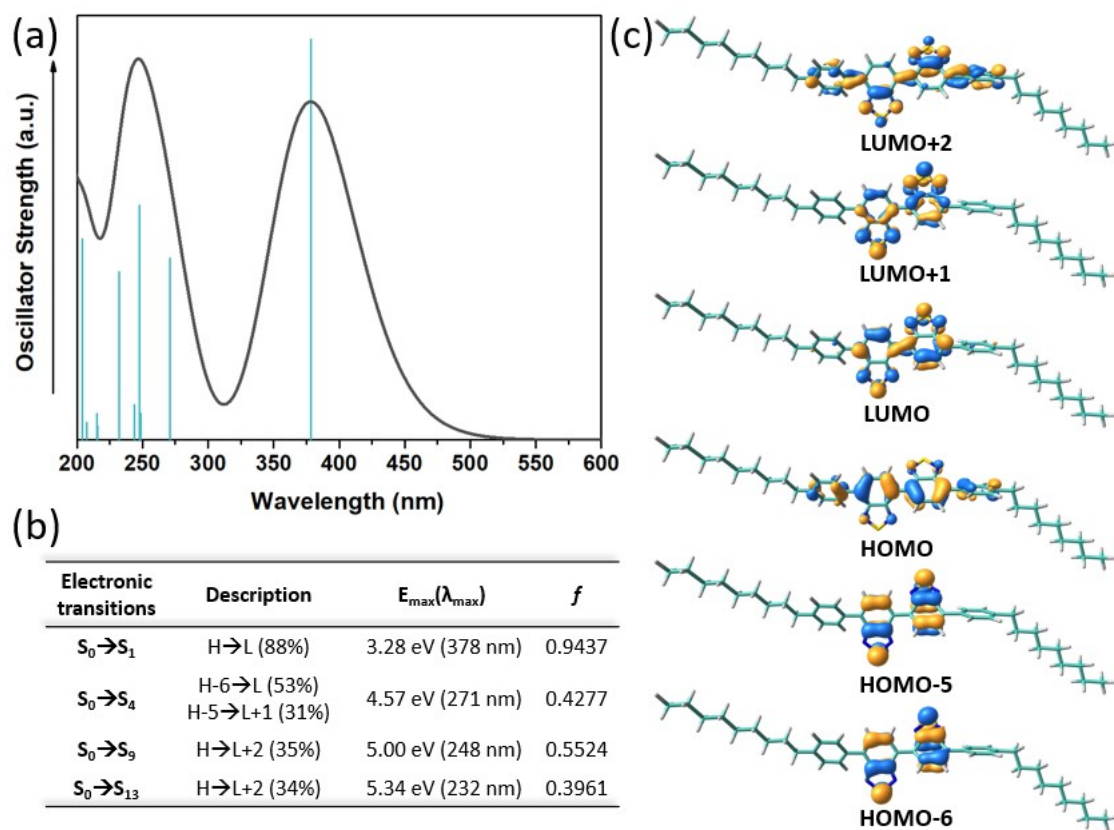


Figure S16. (a) Simulated absorption spectrum of an isolated **B3** molecule obtained from TD-DFT calculations at the ω B97X-D/6-31G** level, with vertical electronic transitions shown as light blue lines. (b) Summary of the main electronic transitions contributing to the absorption features. (c) Topologies of the molecular orbitals involved in the main electronic transitions.

7. Transition dipole moment analysis

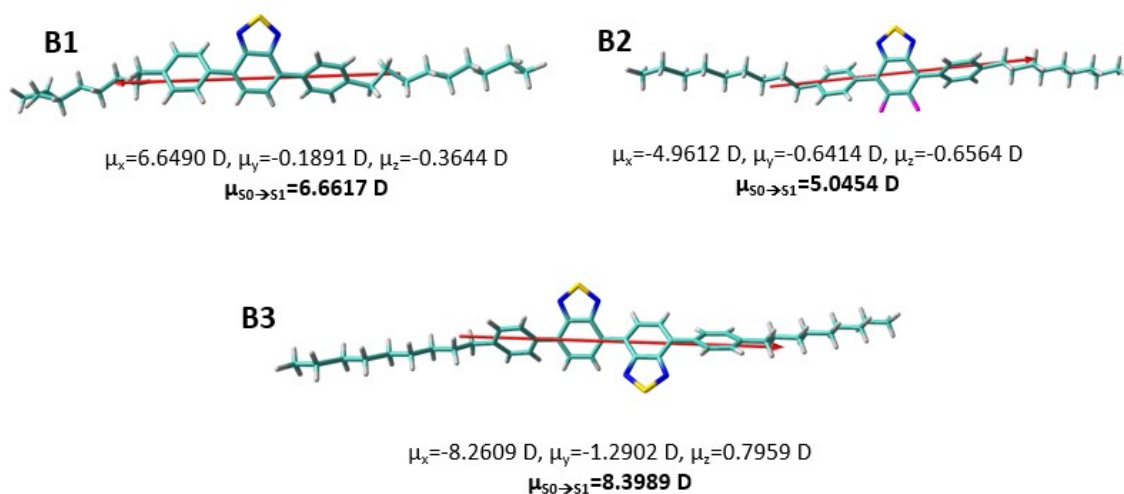


Figure S17. The spatial orientation of the $S_1 \leftarrow S_0$ molecular transition dipole moment for an isolated **B2**, **B2** and **B3** molecules, computed at the ω B97X-D /6-31G** level of theory.

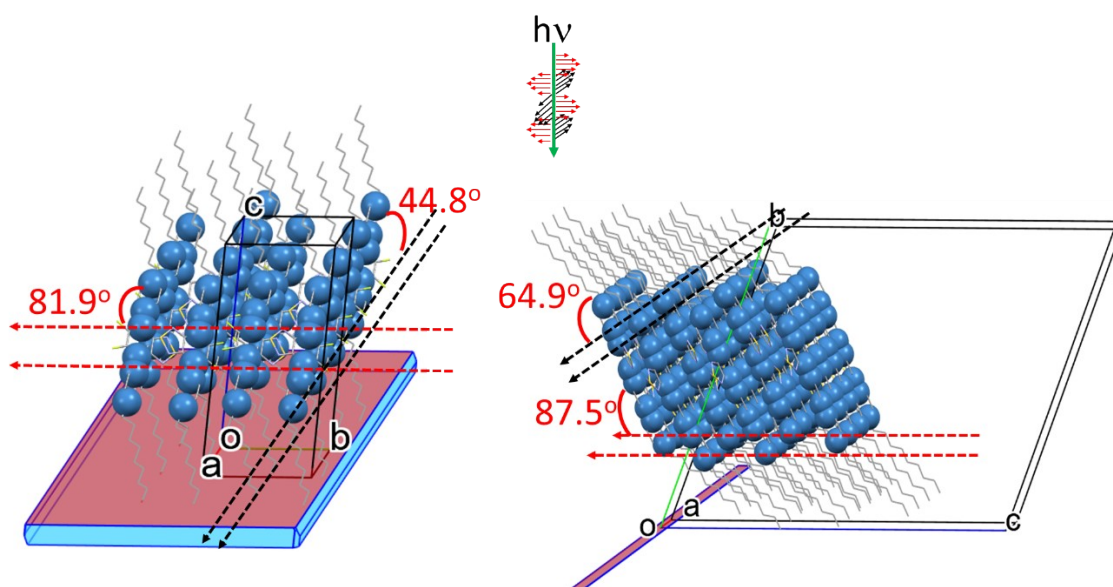


Figure S18. Predicted morphology by Visual Habit program and orientation of molecular transition dipole moment for **B2** and **B3**. The face with the largest surface area is shown in red color. The molecular transition dipole moments are represented by the atoms along the long molecular axis in ball style. The angle formed between the molecular transition dipole moment vector and the irradiated face is indicated. Green arrow is the incident light. Black vectors and waves indicate the longitudinal direction of polarized light relative to the red face. Red vectors and waves indicate the transversal direction of polarized light relative to the red face.

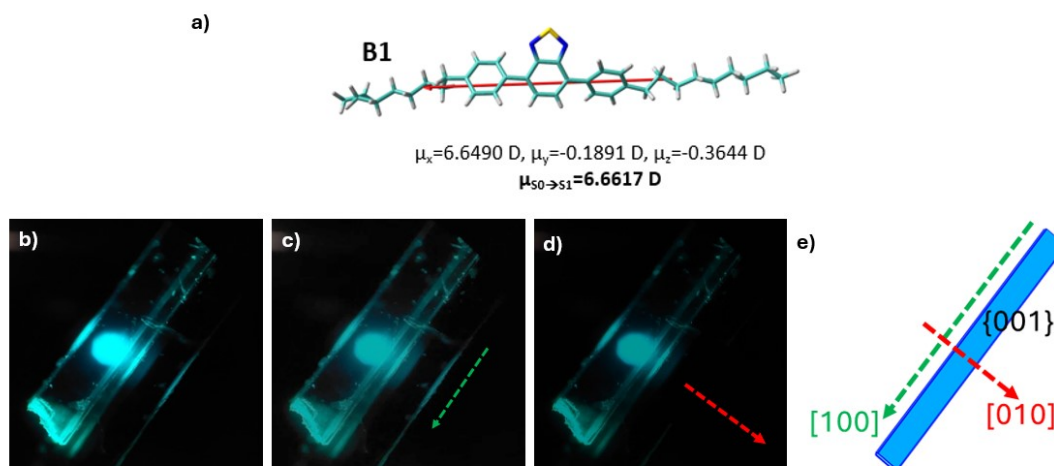


Figure S19. a) The spatial orientation of the S_0 - S_1 transition molecular dipole moment for an isolated **B1** molecule, computed at the ω B97X-D /6-31G** level of theory. b) Confocal microscopy image of the transmitted light without polarization. c) Confocal microscopy image of the transmitted light when the light is polarized in the [100] direction (longitudinal to the {001} face) showed as green arrow. d) Confocal microscopy image of the transmitted light when the light is polarized in the direction [010] (transversal to the {001} face) showed as red arrow. e) Scheme of the different directions and faces in which the polarization has been performed.